Regular Article - Atomic Physics

Positron pair interactions in a nearly free-electron metal

Allen Paine Mills Jr.[a] and Melina Fuentes-Garcia[b]

Department of Physics and Astronomy, University of California, Riverside, CA 92521, USA

Abstract. The electric field surrounding a single positron in a metal is screened by an increase in the local electron density which, in the case of nearly free-electron metals (like Al, Na, etc.), has a radial distribution similar to that of the electron in positronium (Ps). In such metals, a singlet pair of positrons would experience an attractive interaction and at low enough electron densities could possibly form a bound state that is held together by exchange and correlation energies, thus forming structures analogous to that of the positronium molecule (Ps_2), with binding energies of a few tenths of an eV. Such di-positrons could be prevalent at positron densities of around 10^{18} cm^{-3} and, if so, would be evident from an apparent broadening of the sharp step at the Fermi surface in measurements of the electron momentum distribution by the angular correlation of the 2γ annihilation radiation. Even if di-positrons are not directly formed in a metal, optical spectroscopy of Ps_2 formed in vacuum via pairs of positrons simultaneously being emitted from the surface could be applied to the direct measurement of the momentum distribution of Cooper pairs. If they exist, di-positrons in metals would yield interesting information about electron and positron interactions and at very high densities might allow the study of a di-positron Bose–Einstein condensate immersed in an electron gas.

1 Introduction

Positronium (Ps) is the hydrogen-like bound state of an electron and its positron antiparticle. The ground state of Ps is split into a singlet state with a mean lifetime of 125 ps for decay into two 511 keV photons and a triplet state with a 142 ns mean lifetime for decay into three photons with total energy of 1022 keV [1,2]. Positrons have been used to measure the properties of materials since the 1950s [3], with progress being linked to the greater understanding of the positron as a probe. An early example was the need to understand how a positron in its lowest energy state interacts with the electrons of a metal. The Drude–Sommerfeld free-electron model [4], in which the interaction between the ions of a metal and the valence electrons is largely neglected (equivalent to smoothing the ion charge distribution out to form the fictitious metal "jellium" [5]), was very successful in explaining the Wiedemann–Franz law, the Seebeck coefficient, and other properties of real metals. However, the free-electron model was very bad at explaining positron annihilation rates in metals. This problem was rectified by Ferrell, who realized that it is not the average electron density, but the higher actual density at the location of the positron, that determines the annihilation rate [6]. Since that time, ever more sophisticated theories [7–20] have explained the measured annihilation lifetimes of positrons in simple metals [21,22]. These and other theories have also explained, and permitted correction for, small distortions that arise in angular correlation of annihilation radiation (ACAR) measurements [23] of electron momentum densities in crystals [24–28], to the point where the precision and sensitivity of this method are primarily limited by the available positron sources and gamma ray detectors.

2 Di-positrons

With this in mind, it is interesting to consider a new regime in the study of positrons in metals, in which more than one positron is involved in the interactions [29]. Few-nanosecond bursts of slow positrons with areal densities of 10^{11} cm^{-2} have been achieved [30], and it should be possible to implant short bursts of positrons into a metallic target at high instantaneous currents such that the peak density of thermalized positrons is greater than 10^{18} cm^{-3}. This would be sufficient for there to be a significant probability of two positrons interacting with each other over the course of a typical $\sim$ 100 ps lifetime if the cross section for such interaction is $\sim 10^{-16}$ cm^2. One such possible interaction

[a] e-mail: apmjr@ucr.edu (corresponding author)

[b] e-mail: mfuen005@ucr.edu

in a free electron gas of sufficiently low density would be the formation of bound states containing a pair of positrons. These di-positron states would be analogous to Ps_2 molecules [31,32] in vacuum and in insulating crystals, and to bi-excitons [33] in semiconductors, but for the fact that the binding electrons would be part of a continuum of electron states in a metal. Boronski and Nieminen [34], referring to Brinkman and Rice [35], state that (1) Ps_2 molecules will form in an ideal <u>neutral</u> electron–positron e^+–e^- plasma at sufficiently low electron densities such that $r_s > 13.8$, where the dimensionless Wigner–Seitz radius is $r_s = [3/(4\pi n_- a_0^3)]^{1/3}$ with $n_-(n_+)$ being the electron (positron) number density and a_0 being the Bohr radius, and that (2) for $9.8 < r_s < 13.8$, only isolated bound e^+–e^- pairs (Ps), and not Ps_2 molecules, can exist. In the latter range of r_s, there will still be an attractive interaction between two e^+–e^- pairs, but no bound state exists in a neutral e^+–e^- plasma.

A further result of the Boronski–Nieminen two-component density functional theory for e^+–e^- systems in the case of equal electron and positron densities [34] is that in the metallic phase for $3.6 < r_s < 9.8$ there is a minimum in the e^+–e^- correlation energy at $r_s \approx 4$ which is no more than 0.022 Ry $= 0.36$ eV per e^+–e^- pair greater than the threshold for the molecular phase. While this energy deficit is 1.6 times the binding energy of the Ps_2 molecule in vacuum (0.218 eV per e^+–e^- pair [36,37]), the di-positron dissociation energy per pair could be this much larger if the e^+–e^- effective mass ratio were significantly different from 1, or if the lighter of the two effective masses were larger than about 1.6 times the free-electron mass. The latter in fact could be the case given some of the measured values of the positron effective mass ratios, $m^*/m_e = 1.6 \pm 0.1$ for K, 1.55 ± 0.1 for Na, 1.2 ± 0.1 for Mg, and 1.3 ± 0.1 for Al [38]. On the other hand, no definitive conclusions can be made since the measurements may not represent the relevant effective masses which could be some combination of the band effective masses and the renormalized effective masses due to e^+–e^- and e^+–e^- interactions. [39–41].

These calculations do not suggest that di-positron states can exist in a system having equal densities of electrons and positrons. However, they do not necessarily rule out their existence for systems with $n_- \gg n_+$ for which the Fermi energy of the positron system will be negligible. It is therefore reasonable that we try to learn something about di-positrons in metals in anticipation of possible difficulties or advantages that might be encountered in certain proposed experiments that would require producing high densities of positrons in metals. Examples include making high-density positron beams for single-shot [42] positron microscopy [43–46], or increasing the polarization of positron beams for efficient production of Ps Bose–Einstein condensates [47,48], or for measuring spin-resolved band structures [49]. We therefore attempt to estimate the stability of di-positrons in metals based on existing experiments and calculations on the positron ground state in a metal.

3 Di-positron stability

To a good approximation, a single positron in an electron gas will be correlated with at most two electrons in the lowest energy nodeless $1S$-like orbitals relative to the positron. Any further correlated electrons would need to have much larger kinetic energies due to the requirements of wave function orthogonality dictated by the Pauli exclusion principle. Close to the positron, these $1S$-like orbitals will necessarily be similar to the wave function of a free ground state Ps atom which has electron number density

$$\rho(\mathbf{r}) = \frac{1}{4\pi} \left(\frac{1}{a_{Ps}} \right)^3 4 \exp \left\{ \frac{-2r}{a_{Ps}} \right\} \qquad (1)$$

where $\mathbf{r}$ is the vector separation of the electron and positron and $a_{Ps} = 2a_0$ is twice the Bohr radius a_0. We note that even for a low-density metal like Na the average electron density is $3/8$ of the central electron density of a free Ps atom, so that this problem is difficult to treat theoretically, having neither very high nor very low electron densities. An informative example of this type of problem for a 2D electron gas is treated in Ref. [50].

Since the radial dependence of the electron density of the screening cloud that surrounds a positron in a metal is very similar to the electron density relative to the center of mass of the positron in Ps, then if two positrons in a relative singlet spin state are near each other in a simple metal there will be a net attraction between them due to the similar van der Waals and exchange degeneracy [51] forces that cause the binding of the vacuum di-positronium molecule, Ps_2 [31,32,37,52]. The electrostatic repulsion of the two positrons and of the two screening clouds will be slightly less on average than the corresponding attraction between the positive and negative charges. Furthermore, since the two positrons are in a state of total spin zero, their wave functions will each expand to fill a larger volume than they would in isolation while maintaining their nodeless quality, thus decreasing their kinetic energy. Assuming the two electron clouds combine to make a state with predominately singlet spins, the net binding energy of the di-positron (e_2^+) state should be roughly the same as the 0.435 eV binding energy of the Ps_2 molecule in vacuum. The screening cloud associated with the two positrons will consist mostly of only a single electron pair since the inclusion of any further electrons in the cloud would be energetically prohibitive due to the need for the second pair to be in a state orthogonal to the first pair. In principle, one might obtain some reasonable quantitative estimates using a jellium e^+–e^- density functional theory to find the ground state in the absence of annihilations.

It is likely that positronium in a sufficiently dense electron gas will not have a singlet–triplet splitting due to the extremely rapid exchange of electron spins. However, the rapid exchange of electron spins does not necessarily preclude the existence of a singlet two positron

state held together by interactions with the electron gas. It is also interesting that the state of a screened positron in a metal or at its surface is rather like a Majorana Fermion since it has spin one-half and no long-ranged charge interaction. At a surface, a screened positron can annihilate with a second screened surface positron of opposite spin by turning into a spin zero Boson, a free Ps_2 molecule emitted into the vacuum. For this to be truly analogous to annihilation, the metal surface would have to be left in its ground state after the annihilation event.[1]

In the next section, the electron density dependence of the measured positron lifetimes and the calculated correlation energies in simple metals on the one hand, and the calculated electron density around positrons in jellium on the other, will emphasize the hydrogenic character of the e^+–e^- wave function in simple metals and thereby support the thesis of this paper: that in the absence of annihilation, a stable di-positron should exist in a sufficiently low-density metal, with the two positrons held together primarily by a singlet pair of electrons in a state that is qualitatively similar to the vacuum di-positronium molecule, Ps_2. This thesis is further supported by reversing the argument that says the positron state in a free-electron gas approaches the vacuum state of Ps or Ps^- as the electron density diminishes: starting with a free Ps_2 molecule in vacuum, gradually increase the jellium density around the Ps_2, thus proving that the perturbed Ps_2 state exists in the midst of an electron gas at sufficiently low electron densities [54,55]. Two further suggestions by an anonymous reviewer are also very interesting, namely that a Ps^--like or a Ps_2-like configuration could (1) have a significant effect on suppressing the need for gradient corrections in bulk local density approximation calculations [20,56] and (2) help explain the increase in the Ps emission yield from a tungsten surface caused by coating the surface with a low electron density Na layer [57].

4 Single positron states in simple metals and the di-positron

Figure 1a shows measurements of the positron annihilation rates γ for seven simple metals [21,22] as a function of the dimensionless Wigner–Seitz radius r_s. Note that the decay rate for Al is from a measurement on a carefully annealed single crystal [22] such that the positron lifetime is not affected by the longer lifetimes of positrons trapped in dislocations [58] and vacancies [59] in imperfectly annealed samples. In the other samples, the positrons decayed with a single decay rate implying the absence of crystalline disorder. The decay rates plotted in Fig. 1a follow a well-defined curve that has been the subject of an analysis by Seeger and Banhart [12]. As often noted, the measurements suggest that as

---

[1] A sufficiently energetic spin-1 screened positron pair at a surface could annihilate into the $L = 1$ excited state of Ps_2 molecule [53].
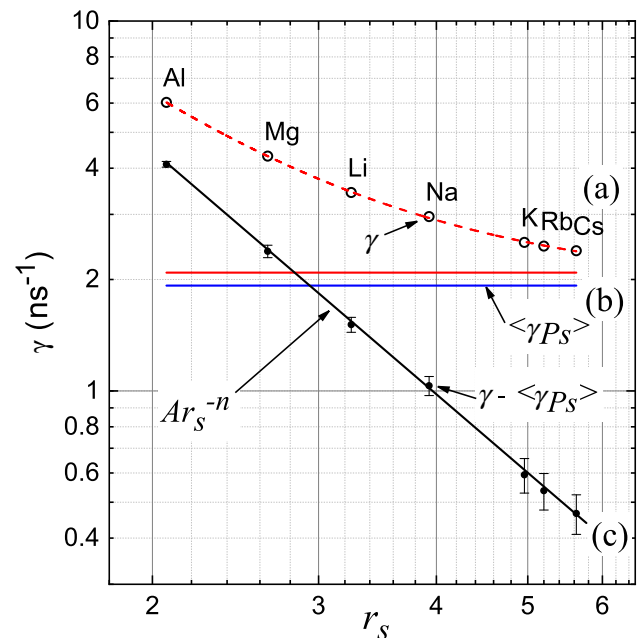

Fig. 1 **a** Measured positron decay rates γ as a function of r_s for the alkali metals and magnesium [21], and for annealed single-crystal Al [22]. The error flags are contained within the plotted circles. The dashed curve is a fit to the measured points using a power law plus a constant. **b** Blue line: Asymptotic spin-averaged positronium decay rate $\langle \gamma_{Ps} \rangle$ from the dashed curve fitted in (**a**); red line: measured Ps^- decay rate. **c** The data of (**a**) minus the constant $\langle \gamma_{Ps} \rangle$ [blue line from (**b**)] fitted using only a power law

$r_s \to \infty$ the decay rate is approaching the spin-averaged free Ps decay rate $\langle \gamma_{Ps} \rangle = (1.998 \pm 0.005)$ ns^{-1} [60] or possibly the Ps^- decay rate indicated by the horizontal red line in Fig. 1b. The dashed curve of Fig. 1a is a fit to the measurements using a curve of the form used by Seeger and Banhart [12]

$$\gamma = A r_s^{-n} + b \qquad (2)$$

which yields $A = (20.12 \pm 0.60)$ ns^{-1}, $n = 2.188 \pm 0.048$, and $b = (1.926 \pm 0.033)$ ns^{-1}, with a reduced chi-squared 0.0748. The rate b (blue line of Fig. 1b) is about 2 standard deviations less than the expected rate for a free spin-averaged Ps atom [12] and 5 standard deviations less than the expectation [6] that the low-density limit of the annihilation rate should be the (2.0875 ± 0.0050) ns^{-1} [61] Ps^- annihilation rate [62]. Following Seeger and Banhart [12], the functional form of $\gamma(r_s)$ in Fig. 1a is made visually apparent by subtracting the fitted limiting rate $b = 1.926$ ns^{-1} (blue line) from the measurements as shown in Fig. 1c.

The value for n from the measurements on seven free-electron-like metals is in reasonable agreement with Ref. [12] which finds $n = 2.43$ fits the metals of Fig. 1 plus 12 others which are considered less free-electron-like and 3 semiconductors. We note that the smallness of the reduced chi-square (0.0748) of the fitted curve in Fig. 1 is likely due to the assignment [21] of a system-

atic error of $\pm$ 2% to the time calibration, which would render the fitted value of parameter b in Eq. 2 statistically consistent with the 1.998 ns^{-1} spin-averaged free Ps annihilation rate.

We now interpret the curves of Fig. 1 based on a toy model of a positronium negative ion in an electron gas, in which the first of its two relative singlet spin state electrons is bound to the positron in an unperturbed Ps 1S-like ground-state wave function annihilating at the constant r_s-independent spin-averaged rate $\langle\gamma_{Ps}\rangle$, horizontal blue line (b). The other electron, curve (c), is bound to the positron in a second 1S-like state with effective binding energy

$$E_0 = \frac{1}{3}\alpha^2 m_e c^2 a_0 \pi^{\frac{1}{3}} \rho(0)^{\frac{1}{3}} \qquad (3)$$

where α is the fine structure constant, c is the speed of light, a_0 is the Bohr radius, and $\rho(0)$ is the central density of the hydrogen-like wave function of the second electron at the location of the positron. We are assuming in Eq. 3 that the reduced mass is $(2/3)m_e$ rather than $(1/2)m_e$ because the positron is inertially connected to the first electron.

We note that the model is a first electron decaying at the spin-averaged decay rate of Ps (nominally 2.00 ns^{-1}) and this is the fit parameter b to the measurements of Fig. 1a which yields $b = (1.926 \pm 0.033)$ ns^{-1}. This is in agreement with the theoretical 2.00 ns^{-1} if we take into account the systematic error estimates of Ref. [21]. The other component is supposed to be that of a weakly bound second electron that gives the power law decreasing rate of curve of Fig. 1c. When this rate becomes less than about 0.08 ns^{-1}, the model fails and the state becomes a mixture of triplet and singlet Ps and Ps$^-$.

The annihilation rate for the second electron is $\gamma - \langle\gamma_{Ps}\rangle$ by construction and is given by the Dirac annihilation rate [63]

$$\gamma - \langle\gamma_{Ps}\rangle = \pi r_0^2 c \rho(0) \qquad (4)$$

Since the previous two expressions are both dependent on the central density $\rho(0)$ of the second electron at the location of the positron, we can eliminate $\rho(0)$ and write a relation between E_0 and $\gamma - \langle\gamma_{Ps}\rangle$:

$$E_0 = \frac{1}{3}\alpha^2 m_e c^2 a_0 \pi^{\frac{1}{3}} \left(\frac{\gamma - \langle\gamma_{Ps}\rangle}{\pi r_0^2 c}\right)^{\frac{1}{3}} \qquad (5)$$

The factor $1/3$ is because the effective mass of the e$^+$–e$^-$ "nucleus" is $(2/3)m_e$. Using Eq. 2, we then express the effective binding energy in terms of r_s:

$$E_0 = \frac{1}{3}\alpha^2 m_e c^2 a_0 \left(\frac{A}{r_0^2 c}\right)^{\frac{1}{3}} r_s^{-\frac{n}{3}} = 0.718 r_s^{-\frac{n}{3}} \text{Ry} \qquad (6)$$

Remarkably, the exponent of r_s using the value of n from the fit in Eq. 2 is

$$-\frac{n}{3} = -0.729 \pm 0.016 \approx -\frac{3}{4} \qquad (7)$$

Thus, E_0 has the same dependence on r_s as the leading term in Ferrell's correlation energy[2]

$$\Delta E = -1.793 r_s^{-\frac{3}{4}} \text{Ry} \qquad (8)$$

so that we have approximately

$$\Delta E = -2.497 E_0 \qquad (9)$$

If we attribute the factor of 2.5 difference between the Ferrell correlation energy and the effective binding energy of the second electron to local enhancement of the electron density in the vicinity of the positron, we could say that curve of Fig. 1c represents the decay of the weakly bound electron of a Ps$^-$ like entity, while the constant line of Fig. 1b represents the constant decay rate of a tightly bound spin-averaged electron component of the same entity. Thus, the sum of the two annihilation rates, a density-independent rate which happens to be nearly equal to the spin-averaged annihilation rate of a ground state free Ps atom (b) and a rate (c) that decreases as a negative power of r_s and is attributed to the second electron of a positronium negative ion in a 1S state, precisely reproduces the measurements in Fig. 1a. This model suggests that the state of a screened positron in a simple metal is not qualitatively different from ordinary Ps$^-$. This conclusion is supported by the comparison of the calculated electron densities for free Ps and the screening electrons around a positron in an ideal metal with $r_s = 2$ and 4 in Fig. 2 [12,14].

The considerations of this section thus support the Ps$^-$-like nature of the positron state in a simple metal and also point to the stability of a Ps$_2$-like state (a di-positron) at positron densities significantly less than the electron densities so that the system is not simply a neutral e$^+$–e$^-$ plasma. In the state we are speaking of the two positrons would share a singlet pair of electrons. Since the annihilation rate of a vacuum Ps$_2$ into two photons plus an e$^+$–e$^-$ pair is 4.4386×10^9 s^{-1} [64], the annihilation rate per positron is 2.2193×10^9 s^{-1}, about 10% greater than the rate of Fig. 1b. Evidence for the existence of di-positrons would be an increase in the annihilation rate at high positron densities.

Since di-positrons must have zero spin in order for the two positrons to share the same orbital, a sufficiently dense collection of di-positrons at low enough temperature might form a single-component Bose–Einstein

---

[2] Ferrell's equation 35 [6].

condensate (BEC) [65]. If the effective mass of a di-positron is about $6m_e$, the BEC critical temperature at a density of 10^{18} e_2^+ cm^{-3} would be about 5 K. Even if the metallic electrons are in the normal state, a di-positron BEC could be superconducting [66] if the di-positrons are effectively disconnected from the screening electrons. One would also expect surface di-positrons to form from a high-density collection of surface positrons, and that these would form a 2D BEC under appropriate conditions [67]. On the other hand, surface di-positrons might be unstable to immediate emission as Ps$_2$ molecules depending on the di-positron surface state binding energy.

5 Physics of the di-positron state

The di-positron state in an electron gas differs from vacuum Ps$_2$ in that the electrons that bind the di-positron are rapidly exchanging places with the electrons of the Fermi sea, while the positrons constitute a singlet pair. It is interesting to consider the fate of a di-positron when it encounters the surface at the vacuum interface after a dense burst of positrons is implanted into a metal crystal. When an isolated positron dressed in its screening cloud encounters a metal surface, the positron can be emitted as a free Ps atom in vacuum with a maximum kinetic energy equal to the sum of the Ps binding energy, 6.803 eV, minus the electron work function, (4.24 ± 0.02) eV for an Al(111) surface [69], implying a Ps work function $\phi_{Ps} = (-2.56 \pm 0.02)$ eV, in agreement with the measured value (-2.62 ± 0.04) eV [68]. If a di-positron encounters the surface, it can be emitted as Ps$_2$ with kinetic energies up to

$$E_{Ps_2,\max} = -2\phi_{Ps_2} + E_{Ps_2} - E_{e_2^+} \approx 5.2 \text{ eV} \quad (10)$$

where $E_{Ps_2} = 0.435$ eV $\approx E_{e_2^+}$ are the binding energies of free di-positronium (Ps$_2$) and the di-positron (e_2^+), respectively. The 5.2 eV energy corresponds to both emitted electrons leaving holes at the Fermi surface. In the case of direct Ps emission from thermalized low-density positrons in a metal, the total energy of the Ps and its momentum parallel to the metal crystal surface are a direct reflection of the energy and momentum distribution of the Fermi sea electrons [49]. The intensity of the component of the Ps kinetic energy perpendicular to the surface for Al(111) will be proportional to the square root of the emission energy with a sharp step of 10%-90% width equal to about 4 $k_B T$ at the Fermi energy, corresponding to the Ps negative work function, as shown in Fig. 3a. On the other hand, the energy and momentum spectrum of Ps$_2$ emitted into the vacuum will reflect the joint energy–momentum spectrum of the hole pair left behind in the solid concomitantly with the emission event. The Doppler distribution of the single photon excitation spectrum of emitted Ps$_2$ [37,53] originating from bulk di-positrons will exhibit a broad distribution of forward emission kinetic energies schematically shown in Fig. 3c. This will be easily distinguished from Ps$_2$ having its origin in the joining of a pair of surface positrons [70–72] illustrated in Fig. 3b. This Ps$_2$ would be emitted with its velocity perpendicular to the surface and a thermal spread in its parallel momentum and in its total kinetic energy, the latter being the Ps$_2$ binding energy of 0.435 eV minus the energy required to produce vacuum Ps starting from a pair of surface positrons or a surface di-positron.

If the sample is a superconductor and its temperature is below the critical temperature, for example $T_c = 1.2$ K [73] for Al or 7.2 K for Pb, some Ps$_2$
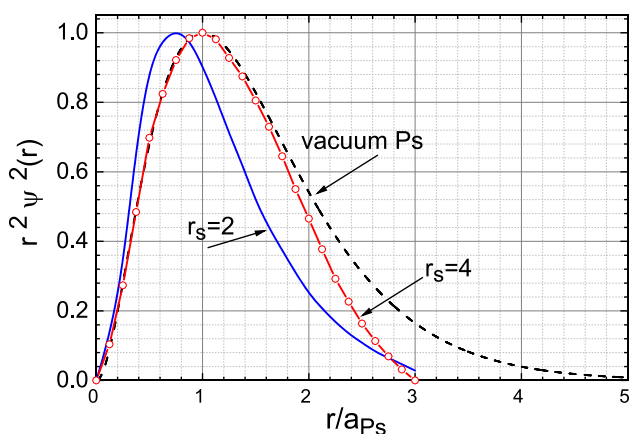
Fig. 2 Peak-normalized radial density $r^2|\Psi(r)|^2$, for vacuum positronium (dashed line). For comparison is shown the electron radial density around a positron in jellium with $r_s = 2$ (blue curve) and 4 (red curve with open circles) according to the calculations of Stachowiak, Fig. 5a, b of Ref. [14]. The quantity a_{Ps} is twice the Bohr radius of hydrogen
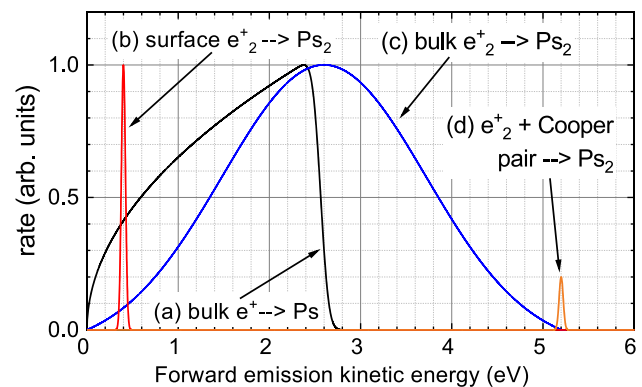
Fig. 3 Estimated forward emission kinetic energy spectra. **a** Ps emission from bulk positrons in Al escaping into the vacuum bound to a conduction electron. The rate of emission is proportional to the density of electron states [68]; **b** dense surface positrons on a hypothetical metal forming Ps$_2$ molecules in vacuum leaving no excitations; **c** Ps$_2$ molecules forming in vacuum directly from di-positrons in Al(111) escaping from the bulk metal. The curves are a self-convolution of curve (**a**); **d** monoenergetic Ps$_2$ molecules forming a di-positron uniting with a Cooper pair for the case of superconducting Al for which $T_c = 1.2$ K

should also be emitted in a peak of thermal width from Ps_2 formation from a di-positron that happens to capture simultaneously the two electrons from a Cooper pair as shown in Fig. 3d. Although this might seem extremely unlikely, the probability for its occurrence should be proportional to the square of the sum of the contributing amplitudes for all the Cooper pairs, since each pair has exactly zero total momentum and all have the same energy. At absolute zero sample temperature, the ratio, α, of the total area of this peak relative to the area of the principal Ps_2 distribution illustrated in Fig. 3c should equal $3\Delta/E_F$. This ratio is the number of electrons that would normally have energies between $E_F - 2\Delta$ and E_F divided by the total number of conduction electrons, where Δ is the energy gap for an ideal conventional superconductor, $\Delta = 1.76\ k_B T_c$ [74]. We would thus have $\alpha \approx 4 \times 10^{-5}$ for Al, $\sim 3 \times 10^{-4}$ for Pb, and possibly 10^{-3} or greater for high-T_c superconductors [75], should the di-positron exist in these materials, which are not simple metals.

There will also be copious emission of Ps^+, positronium plus ions, consisting of two positrons and one electron [31]. Even though they are charged and have a short (479 ± 3) ps mean lifetime [62], one could use the Doppler shift of the Ps^+ Feshbach resonance to measure their emission energy spectra [76,77]. The emission of Ps^+ and Ps_2 by these means will occur at high positron densities with or without the existence of di-positrons, simply because there will be a high density of surface positrons with which to make these objects during the emission of single positrons or Ps from the bulk.

The simplest signature of the presence of di-positrons would be the expected few percent of k_F smearing of the step at the Fermi momentum (k_F) when measured at high positron densities. This could be easily observed by measurements of the angular correlation of the 2γ annihilation radiation (ACAR), where a 1–2% smearing of k_F has been observed simply by heating an Al crystal from 4 to 78 K [38].

6 Increasing the polarization of a positron beam

There is interest in having beams of highly spin-polarized positrons [78,79] for fundamental experiments on beta decay and studies of polarized electrons in solids [80]. Positrons are produced in beta decay with positive helicity $h = v/c$ [81] and a beam of positrons selected from a restricted emission solid angle can have a polarization p along the velocity vector of the beam up to $p_{max} = v_{max}/c = 0.72$ for Na^{22} [82]. A typical slow positron beam using this isotope may have a polarization of about 28% [30]. Since the counting time for a given precision in a polarized positron experiment is proportional to p^{-2}, it is beneficial to have the highest p. An effective method for increasing the polarization p of a beta decay positron source uses an attenuator that preferentially removes the slower particles from the primary beta particle source [80]. This method cannot achieve $p > v_{max}/c$, but using dense positrons could remove this limitation.

The various positron emission processes including those just described are illustrated in Fig. 4, with the key to the symbols being shown in Fig. 4a. Shown in Fig. 4b are the well-known surface pathways for thermalized positrons near a metal surface: (1) slow positron emission [83–86], (2) elastic Ps emission with a near Fermi surface electron leaving a single hole in the Fermi sea [49,68], (3) spontaneous Ps^- ion emission from W and Cs deposited W [87] but not energetically allowed for Al, and (4) formation of a surface positron state [70,71]. Since there is only one pathway for slow positron emission at low densities, process 1 of Fig. 4b, the polarization of the re-emitted positrons will be nearly the same as the polarization of the positrons implanted into the target, neglecting depolarization due to spin-orbit scattering during slowing down of the positrons. On the other hand, at high densities there are pathways, illustrated in processes 2 and 3 of Fig. 4c, that suppress the emission of minority spin positrons due to the build-up of majority spin surface positrons which capture majority spins by the formation of Ps_2, thereby increasing the average polarization of the emitted positrons.

The formation of di-positrons, which will increase the net positron polarization simply by consuming minority spin positrons, will also increase the emitted positron polarization in the following way. The diffusion coefficient for a particle of effective mass m^* and scattering mean free path λ in a solid at temperature T is

$$D = \lambda \sqrt{\frac{kT}{m^*}} \qquad (11)$$

Assuming the scattering cross section and mass for a di-positron are four times those of a positron, the diffusion coefficient would be 25% and the mean diffusion length $L = \sqrt{Dt}$ after a given time t would be 50% of the corresponding L for a single positron. After the implantation of a high-density burst of positrons into a solid, any di-positrons that are formed will therefore lag behind single positrons in their attempt to reach the surface of the solid into which the positrons have been implanted. Since di-positron formation is thus effectively partially immobilizing the minority spin positrons, the net polarization of the positrons reaching the surface will be enhanced. This affords a means to increase the polarization of positrons simply by implanting them at high density into the back of a transmission remoderator foil [88–90]. This assumes that the di-positrons are not forming a BEC so that the ordinary Fick's laws of diffusion apply. The increase in polarization would incur the cost of a reduction in the total number of available positrons. At the same time, the surface will develop a high density of surface positrons with lifetimes about three times longer than in the bulk metal [91]. The surface positron layer will become highly polarized through elimination of minor-
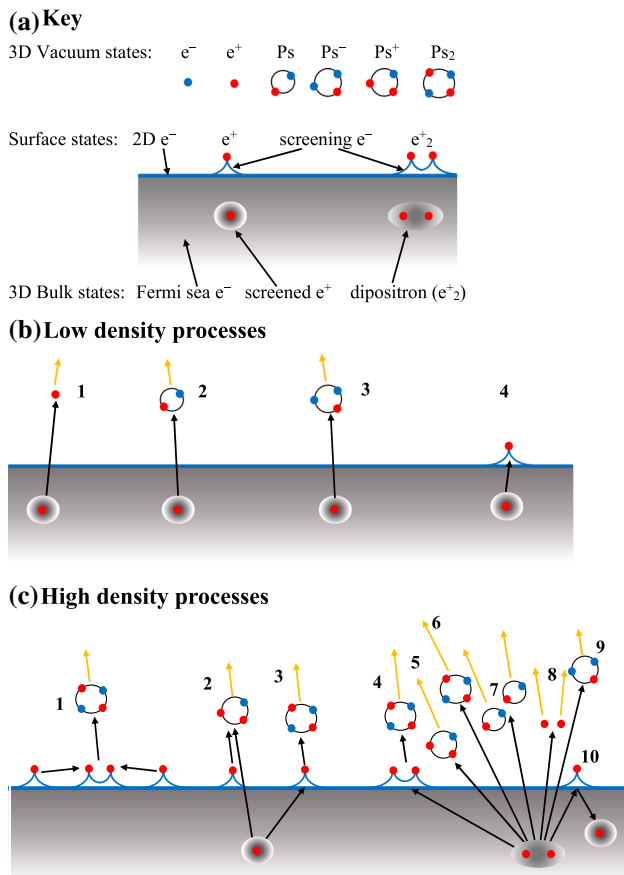
Fig. 4 Some emission processes for dense positrons coming to the surface of a metal. **a** Key to symbols for e^-, e^+, Ps^-, Ps^+, and Ps_2; for the 2D e^- sheet, the surface e^+ and the surface di-positron; and for the Fermi sea, a screened e^+, and a screened di-positron in the bulk. **b** Various surface processes at low positron densities: (1) slow positron emission, (2) Ps emission with a near Fermi surface electron, (3) Ps^- ion emission (likely not energetically allowed for Al), and (4) formation of a surface positron state. **c** Some surface processes at high positron densities: (1) Two surface positrons are shown forming a surface di-positron that is spontaneously emitted from the surface. Next, a bulk screened positron encounters a surface positron, forming (2) a Ps^+ ion and (3) a Ps_2 molecule in vacuum. Finally, a bulk di-positron forms (4) a surface di-positron, (5) a Ps^+ ion, (6) a Ps_2 molecule in vacuum, (7) a pair of Ps atoms in vacuum, (8) a simultaneously emitted pair of slow positrons, (9) a Ps^- ion (likely not energetically allowed for Al), and (10) a single screened positron surface state with the other positron left in the bulk, one of several processes that have the same outcome as the low-density processes in (**b**)

ity spin positrons via the formation of di-positron surface states or the emission of Ps_2 molecules. The dense surface layer of majority spin positrons thus will act as a sieve that consumes minority spin positrons, suppressing their emission as bare particles via processes 2 and 3 of Fig. 4c.

This method for increasing the polarization of a slow positron beam has the advantage of effectively includ-

ing a stage of brightness enhancement, since the volume of phase space occupied by the re-emitted positrons is far less than that of the incoming focused energetic positrons [92] and also would not be limited to a single stage of polarization enhancement.

7 Conclusions

The well-known screening of the electric field of a single positron by conduction electrons implies that dipositron bound states should exist in the electron gas of an ideal simple metal at sufficiently low densities and that these states could therefore be present given a sufficiently high positron density. Evidence for dipositrons—an apparent smearing of the Fermi surface in momentum space as measured by ACAR [26], an anomalous positron density dependence of the positron diffusion rate, an increase in the two-photon annihilation rate at high positron densities, and the possibility of monoenergetic Ps_2 emission peaks from a superconducting metal surface—could be sought using a combination of presently available positron techniques.

Author contributions

A.P. Mills, Jr. is the main author, and M. Fuentes-Garcia joined in discussions and assisted in the preparation of the manuscript.

Data Availability Statement This manuscript has no associated data in a data repository. [Author's comment: The data in this manuscript was taken from the literature. The individual data points of Fig. 1 were obtained from Ref. [21,22] and the curves were obtained as described in the text, Sect. 4. The curves in Fig. 2 were estimated from figures 5 a and b of Ref. [14]. The data in Fig. 3 was estimated as described in the text, Sect. 5.]

References

1. D.B. Cassidy, Experimental progress in positronium laser physics. Eur. Phys. J. D. **72**, 53 (2018). https:// doi.org/10.1140/epjd/e2018-80721-y

2. P. Moskal, B. Jasińska, E.L. Stepień, S.D. Bass, Positronium in medicine and biology. Nat. Rev. Phys. **1**, 527 (2019). https://doi.org/10.1038/s42254-019-0078-7

3. S. DeBenedetti, C.E. Cowan, W.R. Konneker, H. Primakoff, On the angular distribution of two-photon annihilation radiation. Phys. Rev. **77**, 205 (1950). https:// doi.org/10.1103/PhysRev.77.205

4. A. Sommerfeld, Zur elektronentheorie der metalle auf grund der Fermischen statistik. Z. Phys. **47**, 1 (1928). https://doi.org/10.1007/BF01391052

5. The name "jellium" was coined by Conyers Herring who in 1952 wrote "The fictitious metal consists ...of a medium with a uniform distribution of positive charge – we may call it 'positive jelly' – and a compensating number of electrons. This metal... we may call 'jellium' to distinguish it from real metals such as sodium." Quoted from R.I.G. Hughes [93]

6. R.A. Ferrell, Theory of positron annihilation in solids. Rev. Mod. Phys. **28**, 308 (1956). https://doi.org/10. 1103/RevModPhys.28.308

7. J.P. Carbotte, S. Kahana, Positron annihilation in an interacting electron gas. Phys. Rev. **139**, A213 (1965). https://doi.org/10.1103/PhysRev.139.A213

8. D.N. Lowy, A.D. Jackson, Positron annihilation and electron correlations in metals. Phys. Rev. B. **12**, 1689 (1975). https://doi.org/10.1103/PhysRevB.12.1689

9. J. Arponen, E. Pajanne, The momentum distribution of the positron in an electron gas. J. Phys. C Solid State Phys. **12**, L161 (1979). https://doi.org/10.1088/ 0022-3719/12/4/006

10. E. Boroński, Z. Szotek, H. Stachowiak, Exact solution of the Kahana equation for a positron in an electron gas. Phys. Rev. B. **23**, 1785 (1981). https://doi.org/10. 1103/PhysRevB.23.1785

11. A. Rubaszek, H. Stachowiak, E. Boroński, Z. Szotek, Electron-positron enhancement factors for an electron gas of high density within the Kahana formalism. Phys. Rev. B. **30**, 2490 (1984). https://doi.org/10.1103/ PhysRevB.30.2490

12. A. Seeger, F. Banhart, On the systematics of positron lifetimes in metals. Phys. Status Solidi A. **102**, 171 (1987). https://doi.org/10.1002/pssa.2211020117

13. A. Rubaszek, H. Stachowiak, Self-consistent solution of the Kahana equation for a positron in an electron gas. Phys. Rev. B. **38**, 3846 (1988). https://doi.org/10.1103/ PhysRevB.38.3846

14. H. Stachowiak, Electron-positron interaction in jellium. Phys. Rev. B. **41**, 12522 (1990). https://doi.org/10. 1103/PhysRevB.41.12522

15. I. Nagy, B. Apagyi, K. Ladányi, A Thomas-Fermi-Weizsäcker approach to the total positron annihilation in electron gas. Solid State Commun. **86**, 209 (1993). https://doi.org/10.1016/0038-1098(93)90489-A

16. H. Stachowiak, J. Lach, Positron-annihilation characteristics in an electron gas from low to high densities. Phys. Rev. B. **48**, 9828 (1993). https://doi.org/10.1103/ PhysRevB.48.9828

17. B. Barbiellini, M.J. Puska, T. Korhonen, A. Harju, T. Torsti, R.M. Nieminen, Calculation of positron states and annihilation in solids: A density-gradient-correction scheme. Phys. Rev. B. **53**, 16201 (1996). https://doi. org/10.1103/PhysRevB.53.16201

18. E. Boroński, H. Stachowiak, Positron-electron correlation energy in an electron gas according to the perturbed-hypernetted-chain approximation. Phys. Rev. B. **57**, 6215 (1998). https://doi.org/10.1103/ PhysRevB.57.6215

19. J.M.C. Robles, E. Ogando, F. Plazaola, Positron lifetime calculation for the elements of the periodic table. J. Phys. Condens. Matter. **19**, 176222 (2007). https:// doi.org/10.1088/0953-8984/19/17/176222

20. J. Kuriplach, B. Barbiellini, Improved generalized gradient approximation for positron states in solids. Phys. Rev. B. **89**, 155111 (2014). https://doi.org/10.1103/ PhysRevB.89.155111

21. H. Weisberg, S. Berko, Positron lifetimes in metals. Phys. Rev. **154**, 249 (1967). https://doi.org/10.1103/ PhysRev.154.249

22. R.M.J. Cotterill, K. Petersen, G. Trumpy, J. Traff, Positron lifetimes and trapping probabilities observed separately for vacancies and dislocations in aluminium. J. Phys. F Met. Phys. **2**, 459 (1972). https://doi.org/ 10.1088/0305-4608/2/3/015

23. A.T. Stewart, Angular correlation of photons from positron annihilation in solids. Phys. Rev. **99**, 594 (1955). https://doi.org/10.1103/PhysRev.99.594.2

24. S.M. Kim, A.T. Stewart, J.P. Carbotte, Minimum energy of positrons in metals. Phys. Rev. Lett. **18**, 385 (1967). https://doi.org/10.1103/PhysRevLett.18.385

25. J.P. Carbotte, Positrons in metals, in *Positron Solid-State Physics*, ed. By W. Brandt, A. Dupasquier (North-Holland Publ. Co., Netherlands, 1983), Vol. 83 of *Proc. of the Int. School of Physics "Enrico Fermi"*, pp. 32–63, ISBN 9780444865212. https://inis.iaea.org/search/ search.aspx?orig_q=RN:15034626

26. S. Berko, Momentum density and Fermi-surface measurements in metals by positron annihilation, in *Positron Solid-State Physics*, ed. By W. Brandt, A. Dupasquier (North-Holland Publ. Co., Netherlands, 1983), Vol. 83 of *Proc. of the Int. School of Physics "Enrico Fermi"*, pp. 64–145, ISBN 9780444865212. https://inis.iaea.org/search/search.aspx?orig_q=RN: 15034627

27. P.E. Mijnarends, Electron momentum densities in metals and alloys, in *Positrons in Solids*, ed. By P. Hautojärvi (Springer Berlin Heidelberg, Berlin, 1979), Vol. 12 of *Topics in Current Physics*, pp. 25–88, ISBN 9783642813184. https://link.springer.com/10. 1007/978-3-642-81316-0_2

28. S.B. Dugdale, Life on the edge: A beginner's guide to the Fermi surface. Phys. Scr. **91**, 053009 (2016). https:// doi.org/10.1088/0031-8949/91/5/053009

29. A. Dupasquier, A.P. Mills Jr, R.S. Brusa, eds., *Physics with Many Positrons*, Vol. 174 of *Proc. of the Int. School of Physics "Enrico Fermi"* (IOS Press, Ams-

terdam, 2010), ISBN 9781607506461. https://ebooks.iospress.nl/volume/physics-with-many-positrons

30. D.B. Cassidy, V.E. Meligne, A.P. Mills Jr., Production of a fully spin-polarized ensemble of positronium atoms. Phys. Rev. Lett. **104**, 173401 (2010). https://doi.org/10.1103/PhysRevLett.104.173401

31. J.A. Wheeler, Polyelectrons. Ann. N. Y. Acad. Sci. **48**, 219 (1946). https://doi.org/10.1111/j.1749-6632.1946.tb31764.x

32. E.A. Hylleraas, A. Ore, Binding energy of the positronium molecule. Phys. Rev. **71**, 493 (1947). https://doi.org/10.1103/PhysRev.71.493

33. M.A. Lampert, Mobile and immobile effective-mass-particle complexes in nonmetallic solids. Phys. Rev. Lett. **1**, 450 (1958). https://doi.org/10.1103/PhysRevLett.1.450

34. E. Boroński, R.M. Nieminen, Electron-positron density-functional theory. Phys. Rev. B. **34**, 3820 (1986). https://doi.org/10.1103/PhysRevB.34.3820

35. W.F. Brinkman, T.M. Rice, Electron-hole liquids in semiconductors. Phys. Rev. B. **7**, 1508 (1973). https://doi.org/10.1103/PhysRevB.7.1508

36. J. Usukura, K. Varga, Y. Suzuki, Signature of the existence of the positronium molecule. Phys. Rev. A. **58**, 1918 (1998). https://doi.org/10.1103/PhysRevA.58.1918

37. K. Varga, J. Usukura, Y. Suzuki, Second bound state of the positronium molecule and biexcitons. Phys. Rev. Lett. **80**, 1876 (1998). https://doi.org/10.1103/PhysRevLett.80.1876

38. P. Kubica, A.T. Stewart, Positron motion in metals. Can. J. Phys. **61**, 971 (1983). https://doi.org/10.1139/p83-120

39. D.R. Hamann, Effective mass of positrons in metals. Phys. Rev. **146**, 277 (1966). https://doi.org/10.1103/PhysRev.146.277

40. H.J. Mikeska, Effects of positron phonon interaction in metals. Z. Phys. **232**, 159 (1970). https://doi.org/10.1007/BF01393135

41. M. Hasegawa, On the observed positron effective mass in alkali metals. J. Phys. F Met. Phys. **6**, 1433 (1976). https://doi.org/10.1088/0305-4608/6/8/006

42. D.B. Cassidy, S.H.M. Deng, H.K.M. Tanaka, A.P. Mills Jr., Single shot positron annihilation lifetime spectroscopy. Appl. Phys. Lett. **88**, 194105 (2006). https://doi.org/10.1063/1.2203336

43. L.D. Hulett, J.M. Dale, S. Pendyala, The generation of monoenergetic positrons and some potential applications in materials science. Mat. Sci. Forum. **2**, 133 (1984). https://doi.org/10.4028/www.scientific.net/MSF.2.133

44. J. Van House, A. Rich, First results of a positron microscope. Phys. Rev. Lett. **60**, 169 (1988). https://doi.org/10.1103/PhysRevLett.60.169

45. J. Van House, A. Rich, Surface investigations using the positron reemission microscope. Phys. Rev. Lett. **61**, 488 (1988). https://doi.org/10.1103/PhysRevLett.61.488

46. G.R. Brandes, K.F. Canter, A.P. Mills Jr., Submicron-resolution study of a thin Ni crystal using a brightness-enhanced positron reemission microscope. Phys. Rev. Lett. **61**, 492 (1988). https://doi.org/10.1103/PhysRevLett.61.492

47. A.P. Mills Jr., Positronium Bose-Einstein condensation in liquid ^{4}He bubbles. Phys. Rev. A. **100**, 063615 (2019). https://doi.org/10.1103/PhysRevA.100.063615

48. A.P. Mills Jr., Possible experiments with high density positronium. AIP Conf. Proc. **2182**, 030001 (2019). https://doi.org/10.1063/1.5135824

49. A.C.L. Jones, H.J. Rutbeck-Goldman, T.H. Hisakado, A.M. Piñeiro, H.W.K. Tom, A.P. Mills Jr., B. Barbiellini, J. Kuriplach, Angle-resolved spectroscopy of positronium emission from a Cu(110) surface. Phys. Rev. Lett. **117**, 216402 (2016). https://doi.org/10.1103/PhysRevLett.117.216402

50. V. Huard, R.T. Cox, K. Saminadayar, A. Arnoult, S. Tatarenko, Bound states in optical absorption of semiconductor quantum wells containing a two-dimensional electron gas. Phys. Rev. Lett. **84**, 187 (2000). https://doi.org/10.1103/PhysRevLett.84.187

51. L.I. Schiff, *Quantum Mechanics*, Int. Series in Pure and Applied Physics, 3rd edn. (McGraw-Hill, New York, 1987), p. 449, ISBN 9780070856431. http://113.160.249.209:8080/xmlui/handle/123456789/12794

52. D.B. Cassidy, A.P. Mills Jr., The production of molecular positronium. Nature. **449**, 195 (2007). https://doi.org/10.1038/nature06094

53. D.B. Cassidy, T.H. Hisakado, H.W.K. Tom, A.P. Mills Jr., Optical spectroscopy of molecular positronium. Phys. Rev. Lett. **108**, 133402 (2012). https://doi.org/10.1103/PhysRevLett.108.133402

54. G. Ferrante, Annihilation of positrons from positronium negative ion $e^-e^+e^-$. Phys. Rev. **170**, 76 (1968). https://doi.org/10.1103/PhysRev.170.76

55. D. Bressanini, Internal structure of the positronium ion Ps$^-$. Phys. Rev. A. **104**, 022819 (2021). https://doi.org/10.1103/PhysRevA.104.022819

56. B. Barbiellini, J. Kuriplach, Proposed parameter-free model for interpreting the measured positron annihilation spectra of materials using a generalized gradient approximation. Phys. Rev. Lett. **114**, 147401 (2015). https://doi.org/10.1103/PhysRevLett.114.147401

57. H. Terabe, S. Iida, T. Yamashita, T. Tachibana, B. Barbiellini, K. Wada, I. Mochizuki, A. Yagishita, T. Hyodo, Y. Nagashima, Increase in the positronium emission yield from polycrystalline tungsten surfaces by sodium coating. Surf. Sci. **641**, 68 (2015). https://doi.org/10.1016/j.susc.2015.05.012

58. S. Berko, J.C. Erskine, Angular distribution of annihilation radiation from plastically deformed aluminum. Phys. Rev. Lett. **19**, 307 (1967). https://doi.org/10.1103/PhysRevLett.19.307

59. I.K. MacKenzie, T.L. Khoo, A.B. McDonald, B.T.A. McKee, Temperature dependence of positron mean lives in metals. Phys. Rev. Lett. **19**, 946 (1967). https://doi.org/10.1103/PhysRevLett.19.946

60. Approximately $\frac{1}{4}$ of the singlet decay rate (7.9909 ± 0.0017) ns^{-1}. measured most precisely by A.H. Al-Ramadhan and D.W. Gidley [94]

61. H. Ceeh, C. Hugenschmidt, K. Schreckenbach, S.A. Gärtner, P.G. Thirolf, F. Fleischer, D. Schwalm, Precision measurement of the decay rate of the negative positronium ion Ps$^-$. Phys. Rev. A. **84**, 062508 (2011). https://doi.org/10.1103/PhysRevA.84.062508

62. F. Fleischer, K. Degreif, G. Gwinner, M. Lestinsky, V. Liechtenstein, F. Plenge, D. Schwalm, Measurement of

the decay rate of the negative ion of positronium (Ps⁻). Phys. Rev. Lett. **96**, 063401 (2006). https://doi.org/10.1103/PhysRevLett.96.063401

63. M. Charlton, J.W. Humberston, *Positron Physics*, Vol. 11 of *Cambridge Monographs on Atomic, Molecular, and Chemical Physics* (Cambridge Univ. Press, Cambridge, 2001). p. 264, ISBN 9780521415507

64. A.M. Frolov, Annihilation of electron-positron pairs in the positronium ion Ps⁻ and bipositronium Ps₂. Phys. Rev. A **80**, 014502 (2009). https://doi.org/10.1103/PhysRevA.80.014502

65. M. Combescot, *Excitons and Cooper Pairs: Two Composite Bosons in Many-Body Physics*. 1st edn. (Oxford Univ. Press, New York, 2015), ISBN 9780198753735

66. P. Pulsifer, G. Kalman, Pair-creation collective modes in an electron gas. Phys. Rev. A. **45**, 5820 (1992). https://doi.org/10.1103/PhysRevA.45.5820

67. J. Kasprzak, M. Richard, S. Kundermann, A. Baas, P. Jeambrun, J.M.J. Keeling, F.M. Marchetti, M.H. Szymańska, R. André, J.L. Staehli et al., Bose-Einstein condensation of exciton polaritons. Nature. **443**, 409 (2006). https://doi.org/10.1038/nature05131

68. A.P. Mills Jr., L. Pfeiffer, P.M. Platzman, Positronium velocity spectroscopy of the electronic density of states at a metal surface. Phys. Rev. Lett. **51**, 1085 (1983). https://doi.org/10.1103/PhysRevLett.51.1085

69. J.K. Grepstad, P.O. Gartland, B.J. Slagsvold, Anisotropic work function of clean and smooth low-index faces of aluminium. Surf. Sci. **57**, 348 (1976). https://doi.org/10.1016/0039-6028(76)90187-4

70. K.G. Lynn, Observation of surface traps and vacancy trapping with slow positrons. Phys. Rev. Lett. **43**, 803 (1979). https://doi.org/10.1103/PhysRevLett.43.803

71. A.P. Mills Jr., Thermal activation measurement of positron binding energies at surfaces. Solid State Commun. **31**, 623 (1979). https://doi.org/10.1016/0038-1098(79)90310-7

72. D.B. Cassidy, S.H.M. Deng, A.P. Mills Jr., Evidence for positronium molecule formation at a metal surface. Phys. Rev. A. **76**, 062511 (2007). https://doi.org/10.1103/PhysRevA.76.062511

73. J.F. Cochran, D.E. Mapother, Superconducting transition in aluminum. Phys. Rev. **111**, 132 (1958). https://doi.org/10.1103/PhysRev.111.132

74. N.W. Ashcroft, N.D. Mermin, *Solid State Physics* (Holt, Rinehart and Winston, New York, 1976), p. 744, eq. 34.19, ISBN 9780030839931

75. J.G. Bednorz, K.A. Müller, Possible high T_C superconductivity in the Ba-La-Cu-O system. Z. Phys. B. **64**, 189 (1986). https://doi.org/10.1007/BF01303701

76. J. Botero, C.H. Greene, Resonant photodetachment of the positronium negative ion. Phys. Rev. Lett. **56**, 1366 (1986). https://doi.org/10.1103/PhysRevLett.56.1366

77. A.P. Mills Jr., Cross section for photoionization of the positronium negative ion at the lowest Feshbach resonance. Can. J. Phys. **91**, 751 (2013). https://doi.org/10.1139/cjp-2013-0210

78. L.A. Page, M. Heinberg, Measurement of the longitudinal polarization of positrons emitted by sodium-22. Phys. Rev. **106**, 1220 (1957). https://doi.org/10.1103/PhysRev.106.1220

79. P.W. Zitzewitz, J.C. Van House, A. Rich, D.W. Gidley, Spin polarization of low-energy positron beams. Phys.

Rev. Lett. **43**, 1281 (1979). https://doi.org/10.1103/PhysRevLett.43.1281

80. A. Rich, R.S. Conti, D.W. Gidley, M. Skalsey, J. van House, P.W. Zitzewitz, Production and applications of monoenergetic polarized positron beams. Hyperfine Interact. **44**, 125 (1989). https://doi.org/10.1007/BF02398663

81. J.D. Jackson, S.B. Treiman, H.W. Wyld, Possible tests of time reversal invariance in beta decay. Phys. Rev. **106**, 517 (1957). https://doi.org/10.1103/PhysRev.106.517

82. H. Wenninger, J. Stiewe, H. Leutz, The ²²Na positon spectrum. Nucl. Phys. A. **109**, 561 (1968). https://doi.org/10.1016/0375-9474(68)90027-4

83. D.G. Costello, D.E. Groce, D.F. Herring, J.W. McGowan, Evidence for the negative work function associated with positrons in gold. Phys. Rev. B. **5**, 1433 (1972). https://doi.org/10.1103/PhysRevB.5.1433

84. B.Y. Tong, Negative work function of thermal positrons in metals. Phys. Rev. B. **5**, 1436 (1972). https://doi.org/10.1103/PhysRevB.5.1436

85. S. Pendyala, D. Bartell, F.E. Girouard, J.W. McGowan, Energy distribution of slow positrons diffusing from incomplete *d*-shell transition metals. Phys. Rev. Lett. **33**, 1031 (1974). https://doi.org/10.1103/PhysRevLett.33.1031

86. A.P. Mills Jr., P.M. Platzman, B.L. Brown, Slow-positron emission from metal surfaces. Phys. Rev. Lett. **41**, 1076 (1978). https://doi.org/10.1103/PhysRevLett.41.1076

87. Y. Nagashima, T. Hakodate, A. Miyamoto, K. Michishio, Efficient emission of positronium negative ions from Cs deposited W(100) surfaces. New J. Phys. **10**, 123029 (2008). https://doi.org/10.1088/1367-2630/10/12/123029

88. D.M. Chen, K.G. Lynn, R. Pareja, B. Nielsen, Measurement of positron reemission from thin single-crystal W(100) films. Phys. Rev. B. **31**, 4123 (1985). https://doi.org/10.1103/PhysRevB.31.4123

89. P.J. Schultz, E.M. Gullikson, A.P. Mills Jr., Transmitted positron reemission from a thin single-crystal Ni(100) foil. Phys. Rev. B. **34**, 442 (1986). https://doi.org/10.1103/PhysRevB.34.442

90. Note that one should probably not use a ferromagnetic thin remoderator like Ni at temperatures below the 354°C Curie temperature with longitudinally polarized positrons because they would become depolarized by the transverse magnetic field of the thin Ni film, unless a strong (∼ 1 T) bias field were applied perpendicular to the Ni surface. Alternately one could use transversely polarized positrons and a small transverse bias field

91. K.G. Lynn, W.E. Frieze, P.J. Schultz, Measurement of the positron surface-state lifetime for Al. Phys. Rev. Lett. **52**, 1137 (1984). https://doi.org/10.1103/PhysRevLett.52.1137

92. A.P. Mills Jr., Brightness enhancement of slow positron beams. Appl. Phys. **23**, 189 (1980). https://doi.org/10.1007/BF00899716

93. R.I.G. Hughes, Perspect. Sci. **14**, 457 (2006)

94. A.H. Al-Ramadhan, D.W. Gidley, Phys. Rev. Lett. **72**, 1632 (1994)